Analysis of Crack Propagation in Polyurethane Panels Subject to Cyclic Compressive Buckling

Tim D. Leister[1], Steven M. Cron[2]

[1]École polytechnique, Paris, France
[2]Michelin Americas Research Company, Greenville, South Carolina

Abstract: When a panel of an elastomeric material, such as polyurethane, is subject to large cyclic in-plane displacements which result in cyclic compressive buckling, cracks will be observed to form at the center and edges of the panel. These cracks tend to propagate across the panel in the region of maximum deflection. If the magnitude of the applied cyclic deflection is held constant, the crack growth rate is observed to be nearly a constant over much of the width of the panel. Interestingly, a constant crack growth rate implies that the strain energy release rate is not a function of the crack length. This raises the following question: What are the geometric parameters that influence the crack growth rate for this type of structure? This paper will present a method for evaluating the strain energy release rate in compressively flexed elastomeric panels and present results showing the influence of basic geometric parameters on the strain energy release rate.

Keywords: Polyurethane, Panel, Buckling, Fatigue, Strain Energy Release Rate, J-Integral.

1. Introduction

When flat panels of elastomeric material, such as polyurethane, are forced to buckle under cyclic compressive loading, these panels will have a tendency to form cracks along the region in the panel with the maximum deformation. In certain cases, the cracks will form near the edges and propagate toward the center of the panel. In other cases, the cracks will form near the center and propagate outward toward the edges as shown in Figure 1.

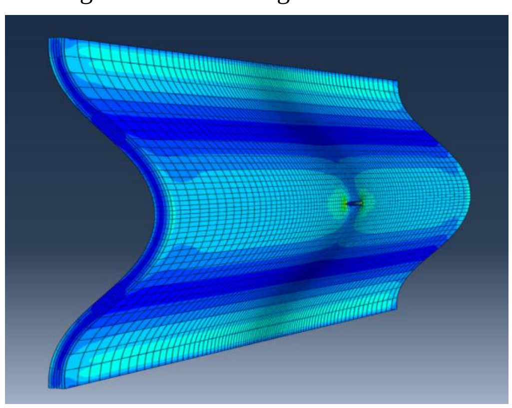

Figure 1. Typical Flexed Finite Element Panel Model with Small Center Crack.

The objective of this study is to gain insight into the factors controlling the crack growth once a crack has been initiated so that criteria for improving panel durability can be proposed. Of particular interest to the authors is a better understanding of the dependence of the crack growth rate on the crack length versus the rate dependence on the panel geometry. We know that in the laboratory we can demonstrate crack length independent crack growth behavior in wide (planar tension) samples with edge cracks as shown in Figure 2a. By contrast, we can also demonstrate crack length dependent behavior in narrow strip samples with edge cracks as shown in Figure 2b.

In a simplistic mathematical form, the well known strain energy release rate (or tearing energy, T) for the planar tension specimen (Figure 2a) is expressed as $T = Wh$, where W is the strain energy density and h is the gage length of the specimen. For the thin strip specimen of Figure 2b, the analogous expression is $T=2kWc$, where k is a strain dependent parameter and c is the crack length (Rivlin, 1953).

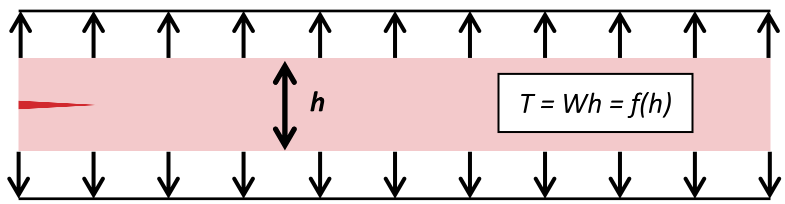

Figure 2a. Planar Tension Specimen Configuration.

If we accept that the crack growth rate for rubbery materials generally follows the behavior shown in Figure 3, for a given level of solicitation in the stable growth region, it is clear that the crack growth rate will be constant (since h is a constant) for the sample in Figure 2a, whereas the rate for the sample in Figure 2b will increase as the crack length, c, increases.

With these two limits of behavior in mind, we want to use simple finite element models to investigate crack length dependency vs. panel geometry dependency in compressively flexed panels. We will accomplish this by evaluating the strain energy release rate (SERR) versus crack length over a range of geometric parameters for our flexed panels.

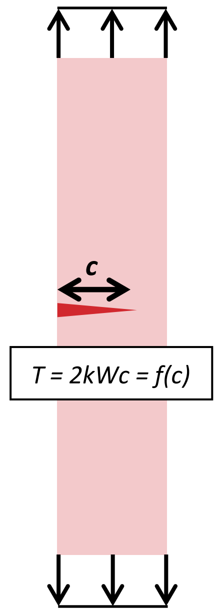

Figure 2b. Thin Strip Specimen with Edge Crack.

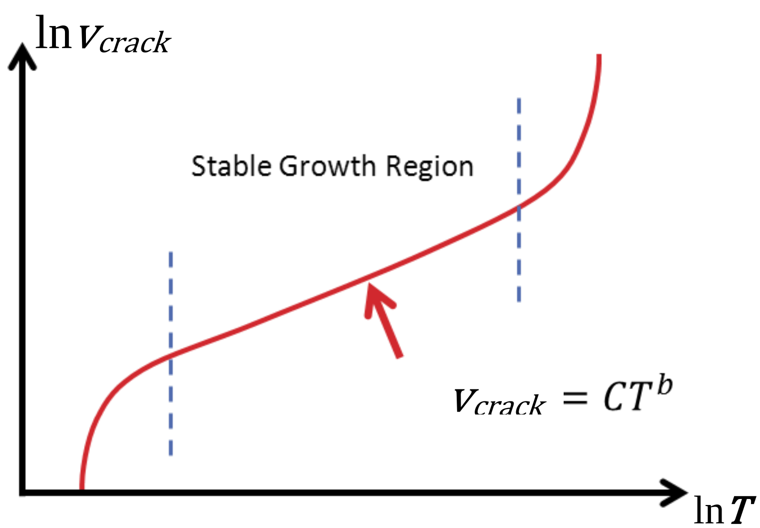

Figure 3. Typical Crack Growth Rate of Rubbery Materials.

2. Strain Energy Release Rate (SERR) Evaluation with FEA

Our approach to calculating the SERR will be a straightforward one. For each panel geometry, we will build a sequence of panel models (aided by the Abaqus python scripting interface) each with an incrementally longer crack. Each model will be loaded to a prescribed deflection and the results used to evaluate the SERR.

Two methods will be used to evaluate the SERR: The Tabular Method and the J-Integral Average Method. The authors chose to use two independent methods as an internal check on results.

2.1 Tabular Method

For the tabular method, we approximate the SERR as:

$$SERR \approx -\frac{\Delta U}{\Delta A} \tag{1}$$

where ΔU and ΔA are the change in total strain energy (`ALLSE`) and crack surface area, respectively, between subsequent crack lengths. While the change in total strain energy is readily available from the finite element results, an accurate evaluation of the change in the crack surface area is more difficult to obtain in structures undergoing large deformations. However, this area can be determined quite accurately by tying a low modulus membrane of constant unit thickness to the new crack surface and using its volume change as a measure of the change in the crack surface area as illustrated in Figure 4.

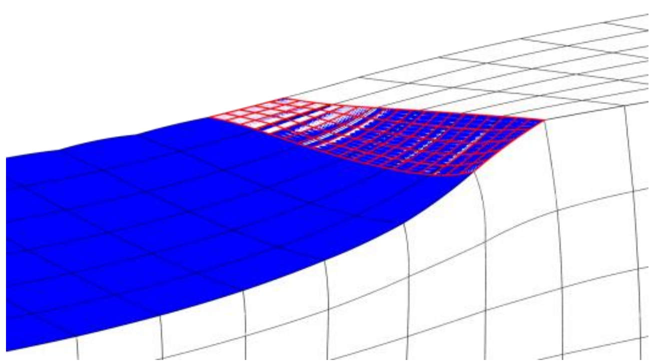

Figure 4. New Crack Surface with Membrane Attached.

2.2 J-Integral Average Method

The SERR for each increment of the crack length was also calculated using the conventional J-integral method available in Abaqus/Standard (Abaqus, 2011). We chose to make this additional calculation of the SERR as a check on the tabular method and as a way to evaluate the advantages and disadvantages of the two methods.

Since we are evaluating the SERR for an explicit crack in a conventional finite element model, we were required to explicitly define the crack front and the virtual crack extension direction directly. In addition, we chose to evaluate the J-integral using 3 contours to give ourselves reasonable assurance that we were obtaining a stable and reliable value for the integral.

Given that our panel structure was undergoing large amounts of bending, the stresses, and therefore the SERR, were non-uniform along the crack front. To accommodate this behavior, the final value for the SERR for each crack increment was taken as the average of the contour integral values for all of the nodes (evenly spaced) along the crack front. In order for this averaging scheme to yield good results, we found that a minimum of 6 second order elements were required through the thickness of the panel.

2.3 Comparison of SERR Calculation Methods

The authors found that by using the techniques described above, the tabular and contour integral methods gave very similar results as seen below in Figure 5.

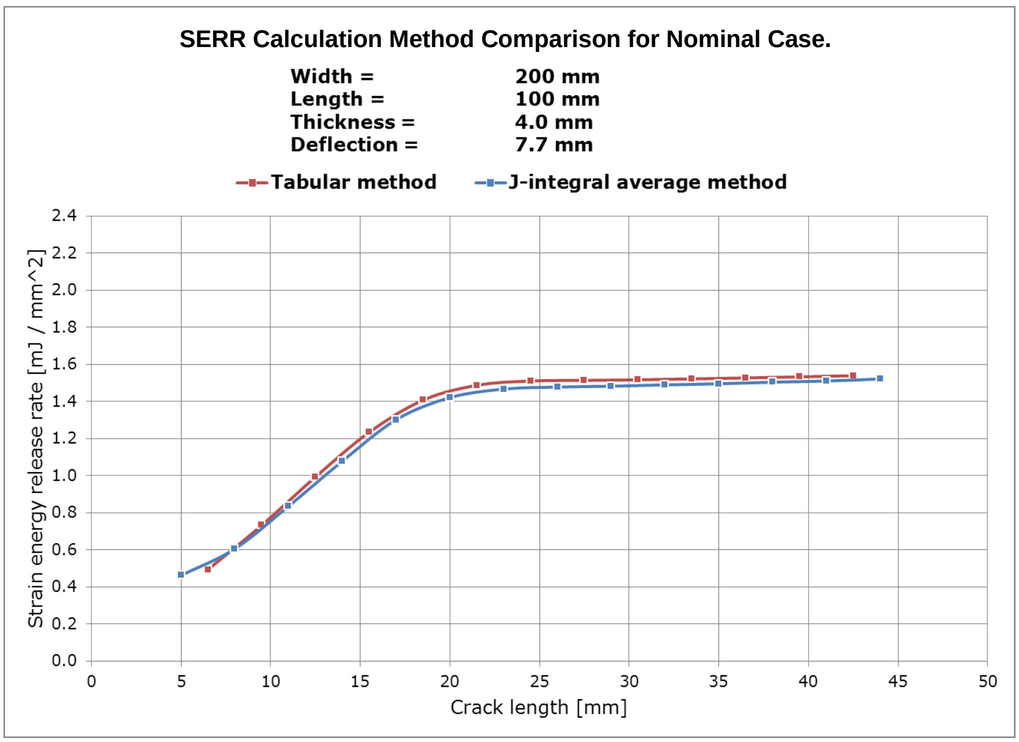

Figure 5. SERR Calculation Method Comparison for Nominal Panel Case.

Our summary of the advantages and disadvantages of the two considered methods are given below:

Table 1. Comparison of Tabular Method vs J-integral Average Method.

Tabular method

+	-
▪ Easy to understand and a very natural approach ▪ Maximum control over SERR calculation algorithm	▪ Cannot be evaluated for a single model and requires automation

J-integral average method

+	-
▪ Could be used for a single model without implementing automation algorithm	▪ Functionality more complicated to understand ▪ Requires many nodes along the crack tip and requires very thin elements

Note that for the remainder of the results presented, only the values from the Tabular method will be plotted even though the values from both methods were computed and compared as a check on results.

3. Modeling of the Cracked Panel

3.1 Panel Crack Geometry

As previously mentioned, the objective of this study was to gain insight into the influence of panel geometry on the relationship between crack length and SERR for compressively flexed elastomeric panels. Specifically, we wanted to investigate the sensitivity of the SERR vs crack length function to:

- panel width,
- panel length,
- panel thickness.

For our study we will define the reference geometry as the following:

- *w = 200 mm* (panel width, distance between free edges)
- *l = 100 mm* (panel length, distance between loaded edges)
- *t = 4 mm* (panel thickness).

The panels were all modeled using lateral symmetry. Quarter symmetry was also considered for the models but was discarded due to difficulties in properly modeling contact between upper and lower crack surfaces.

The crack front in all models was oriented at 45° to the panel face in the plane of the crack as shown in Figure 6. This angle was chosen based on previous calculations that showed this angle gave the most uniform stress distribution along the crack front and also on experimentally observed crack fronts that formed at this angle. Also note that in Figure 6, the top half of the model has been removed for clarity.

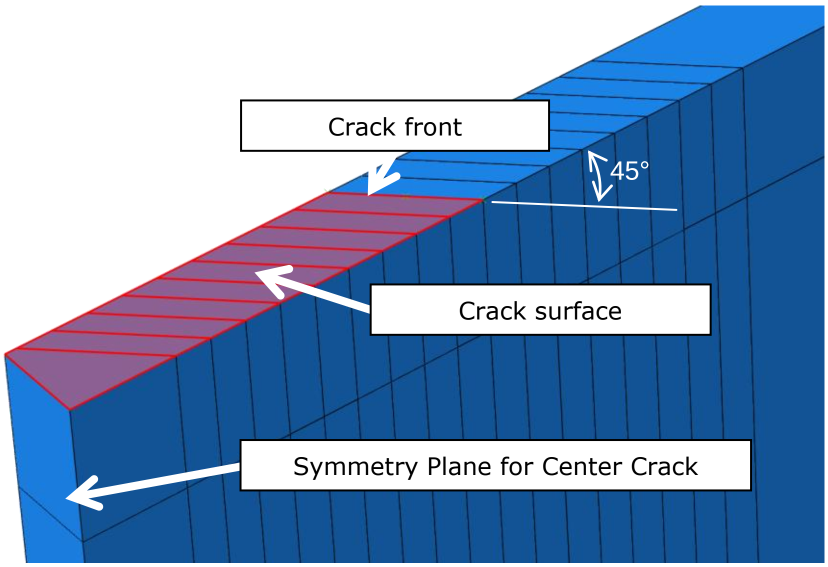

Figure 6. Panel Model Crack and Symmetry Details.

3.2 Loading Sequence

Given that the panels are initially flat, direct compression in the plane of the panel would, in general, result in only in-plane deformation of the panel. In order to induce out-of-plane deformation, some lateral perturbation of the panel must be supplied. In addition, good contact interactions between the two crack faces is best assured by first separating the faces prior to contact. The steps used for the simulations consisted of the following:

- Initial: Undeformed panel
- Step-1: Add traction in order to separate the contact faces.
- Step-2: Add small perturbation to avoid a stability problem
- Step-3: Add pre-compression and initiate contact
- Step-4: Remove perturbation
- Step-5: Vary deflection to different amounts.

The following images in Figure 7 show this deformation history:

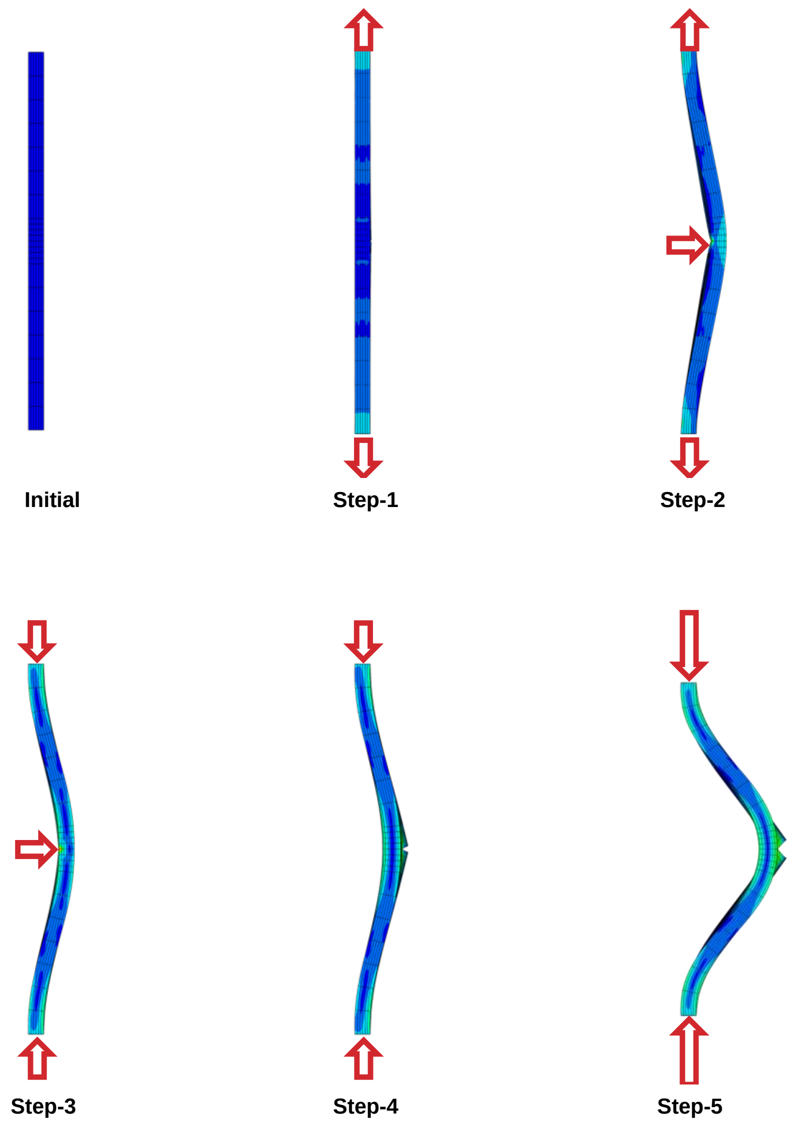

Figure 7. Panel Loading Sequence.

3.3 Deflection Magnitude

Clearly, for any combination of panel geometry and crack length, the SERR will be directly dependent on the magnitude of the compressive deflection applied in Step-5. Since a designer would likely limit the magnitude of the allowable deflection based on some maximum stress, strain, or strain energy density measure, we will, for certain plots, control the deflection based on such a measure. Specifically, in the following sensitivity plots, we will set deflections corresponding to the maximum strain energy density occurring on the convex (tensile) side of the deflected panel. For example, for the reference panel geometry a 7.7 mm compressive deflection corresponds to a 15 psi maximum strain energy density under this scheme. For a panel of a different length or thickness, the deflection would be set at a different level to achieve the same level of strain energy density.

3.4 Materials

All panels were modeled with a Marlow material law fit to experimental uniaxial tension data for Vibrathane B836 at 25C.

4. SERR Sensitivity to Panel Geometry

The following sections will present and discuss the sensitivity of the SERR to variations in panel geometry. Only detailed results for the case of the center crack propagating outward will be presented. A brief discussion of the edge vs. center crack results will be presented thereafter.

4.1 Sensitivity to Panel Width

The first parameter to be examined was the panel width. The width parameter was varied from the nominal (200 mm) by +/- 100 mm. The results are shown in Figure 8. As the five curves are hardly distinguishable, it is clear that the width has no influence on the SERR. This result is not very surprising given that the crack tends to influence only the strain energy density in its nearby vicinity.

Additionally, these curves seem to indicate two different phases of crack propagation behavior. In the first phase at smaller crack lengths, the SERR is clearly a function of crack length and appears to be nearly a linear function. In the second phase, the curve becomes more horizontal, apparently indicating that the SERR is no longer a function of crack length but only a function of panel geometry. These two phases will be typical of all of the results to follow. The factors controlling the slope of the function in phase I and the level in phase II will be of particular interest.

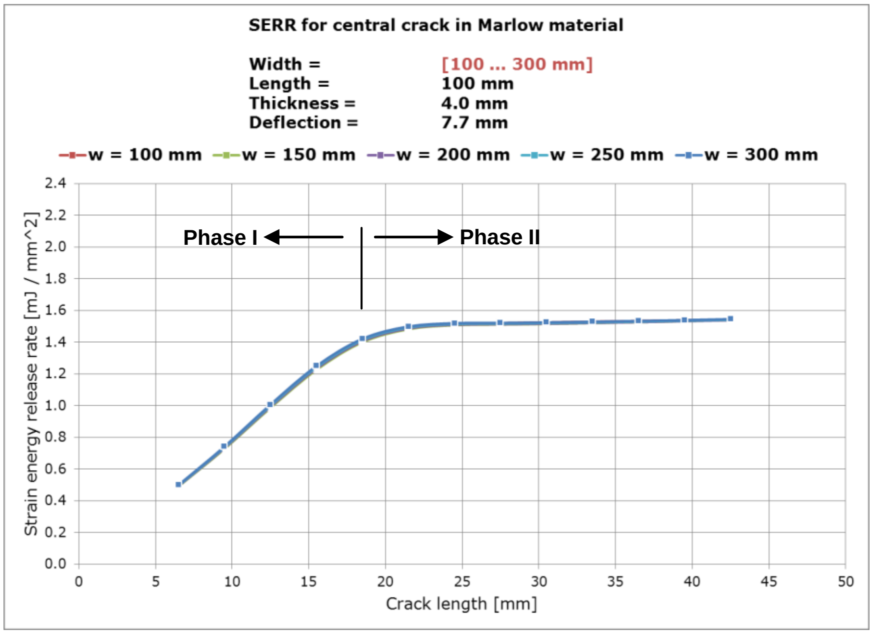

Figure 8. SERR vs. Crack Length for Nominal Case, *Variable Panel Width*.

4.2 Sensitivity to Panel Thickness

The next parameter to be examined was the panel thickness. For this parameter, we varied the thickness as a fraction of the panel length as follows:

$.030 \times l$	$.035 \times l$	$.040 \times l$	$.045 \times l$	$.050 \times l$

Panel width and length were held constant at the nominal values of *200 mm* and *100 mm*, respectively. When we applied an equal deflection to all five models we obtained the results plotted in Figure 9. However, if we normalize the deflections for each model to a peak strain energy density of 15 psi (as explained in section 3.3), we obtain the results plotted in Figure 10. Here we see an indication that the final SERR level in phase II is mainly a function of the peak strain energy density in the panel if the applied deflections are normalized as described. This conclusion will be confirmed in subsequent plots. It should also be noted that the case with the thickest panel ($0.050 \times l$) was prone to numerical difficulties when the crack became longer than 25 mm.

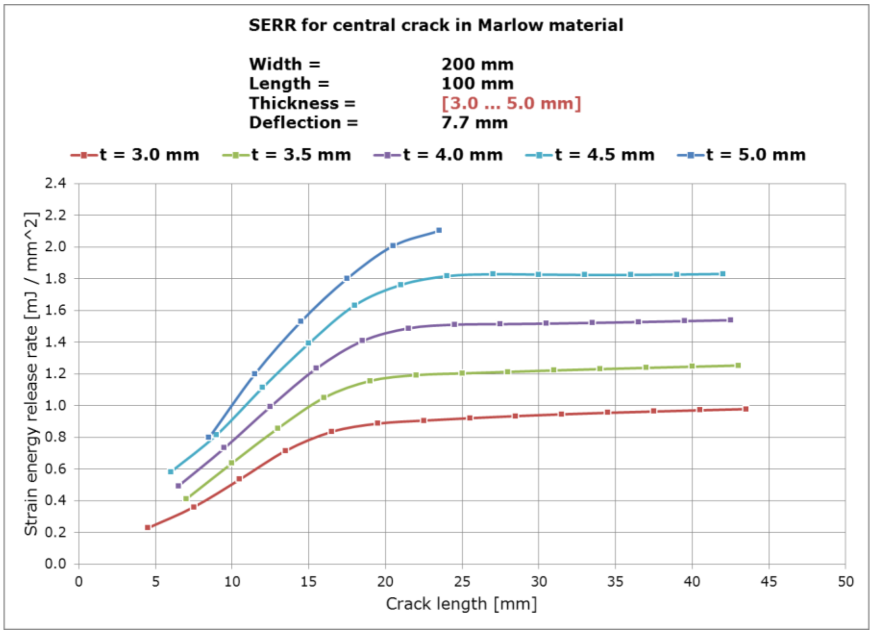

Figure 9. SERR vs. Crack Length, *Variable Thickness (iso-Deflection).*

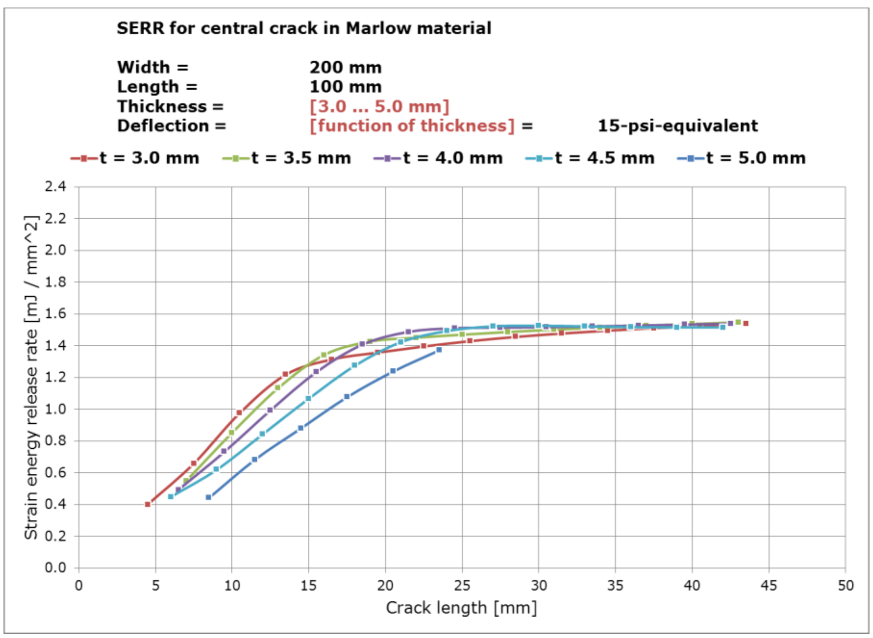

Figure 10. SERR vs. Crack Length, *Var. Thick. (iso-Peak Strain Energy Density).*

4.3 Sensitivity to Panel Length

The final parameter to be varied in the study was the panel length. The length parameter was varied from 50 mm to 150 mm as follows:

50 mm	*75 mm*	*100 mm*	*125 mm*	*150 mm*

For one set of analyses, the panel thickness was held equal to *0.040* × *length* while varying the normalized deflection from *10 psi* to *20 psi*. These results are shown in Figures 11, 12, and 13. Here we see the slope during phase I increasing, for all panel lengths, uniformly as the normalized deflection level is increased. During phase II, the horizontal level is controlled by both panel length and normalized deflection.

For a second set of analyses the normalized deflection was held constant at 15 psi while varying the panel thickness from *0.030* × *length* to *0.045* × *length*. These results are shown in Figures 14, 15, and 16. Here we see the slope during phase I decreasing with increasing panel thickness. This seems counterintuitive at first. However, if we consider that the thicker panels have more strain energy arising from axial (non-bending) compressive stresses that are not released by the crack, the result seems logical. During phase II, the SERR levels are only slightly dependent on panel thickness. In fact, comparing Figures 14 and 15, the levels during phase II are nearly the same.

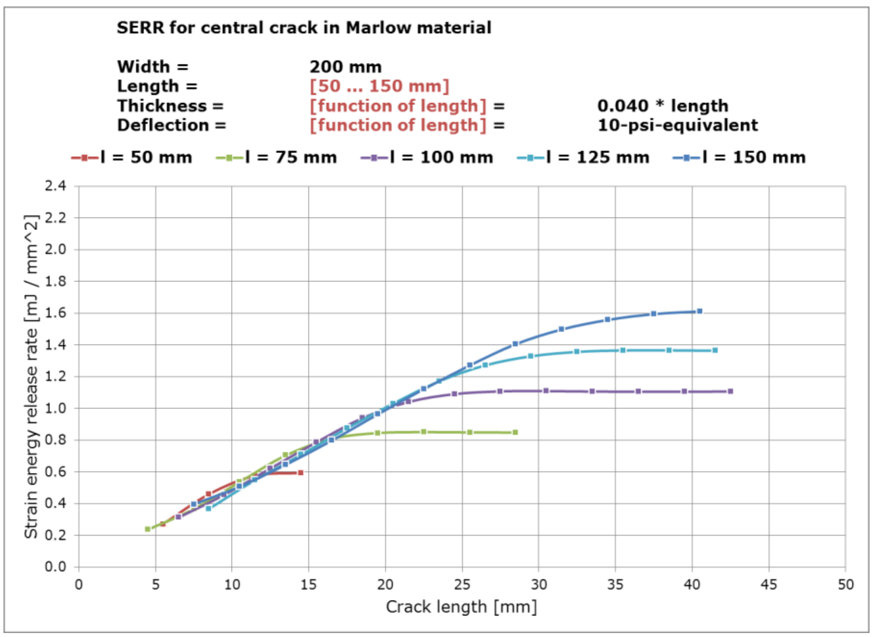

Figure 11. SERR vs. Crack Length, *Variable Length, Def. Norm. - 10-psi.*

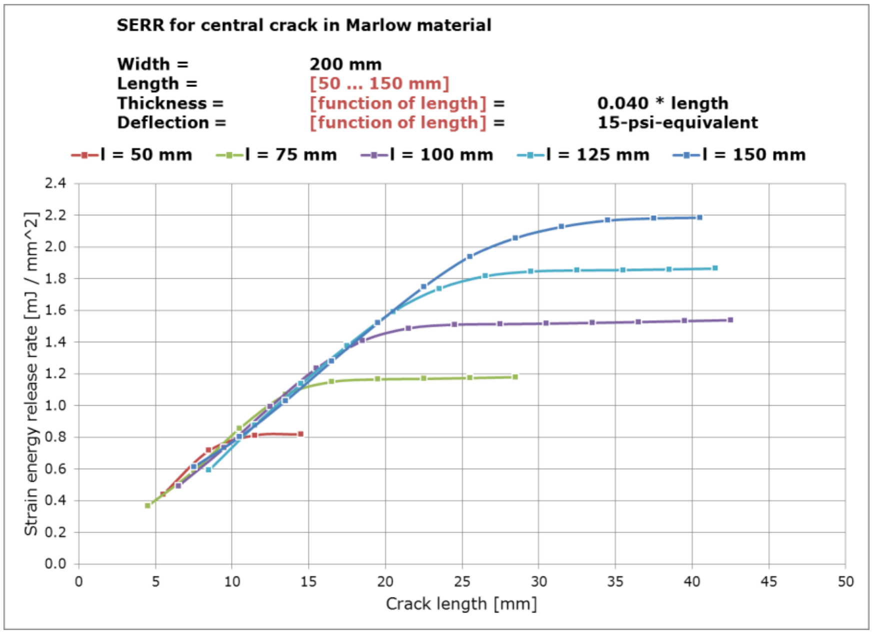

Figure 12. SERR vs. Crack Length, *Variable Length, Def. Norm. - 15-psi.*

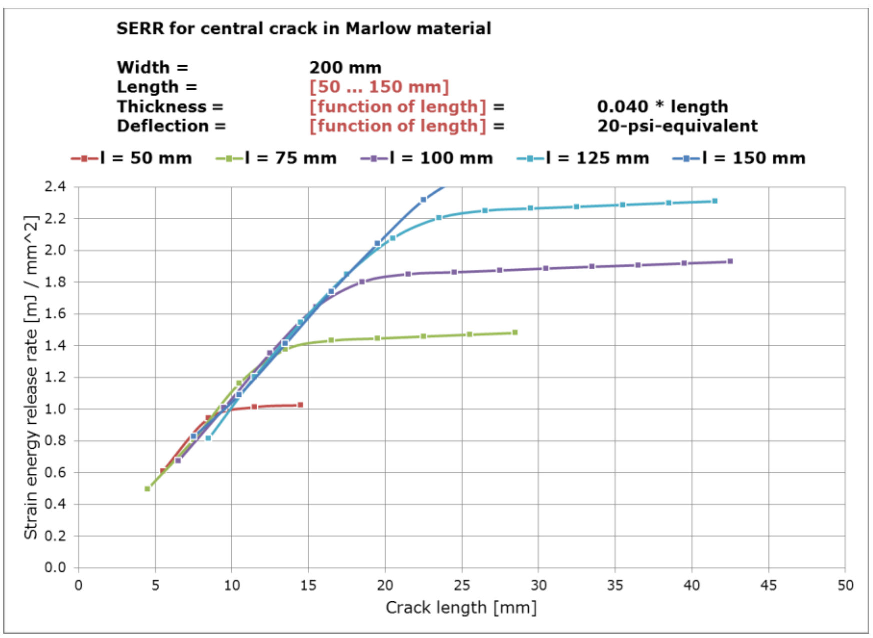

Figure 13. SERR vs. Crack Length, *Variable Length, Def. Norm. - 20-psi.*

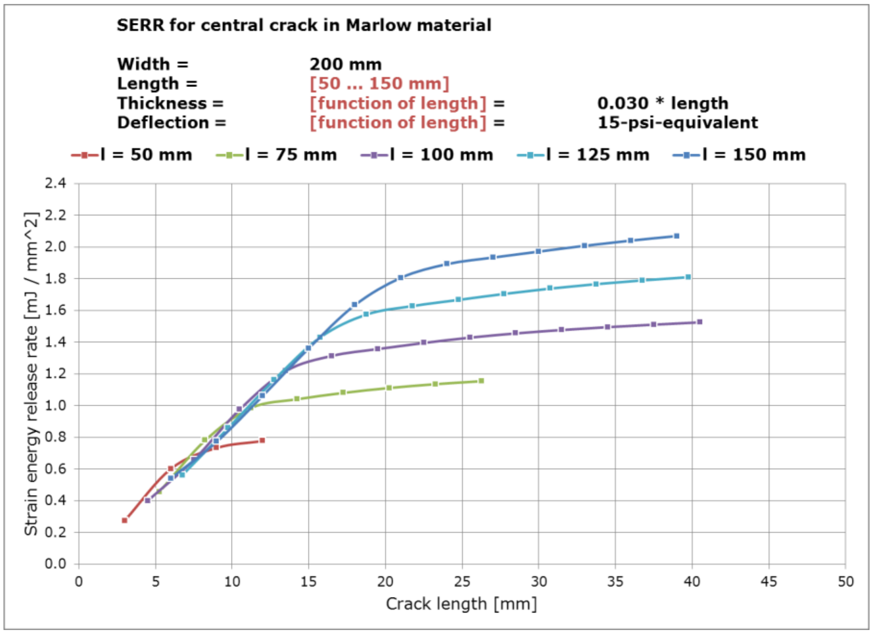

Figure 14. SERR vs. Crack Length, *Variable Length, t = .03*Length.*

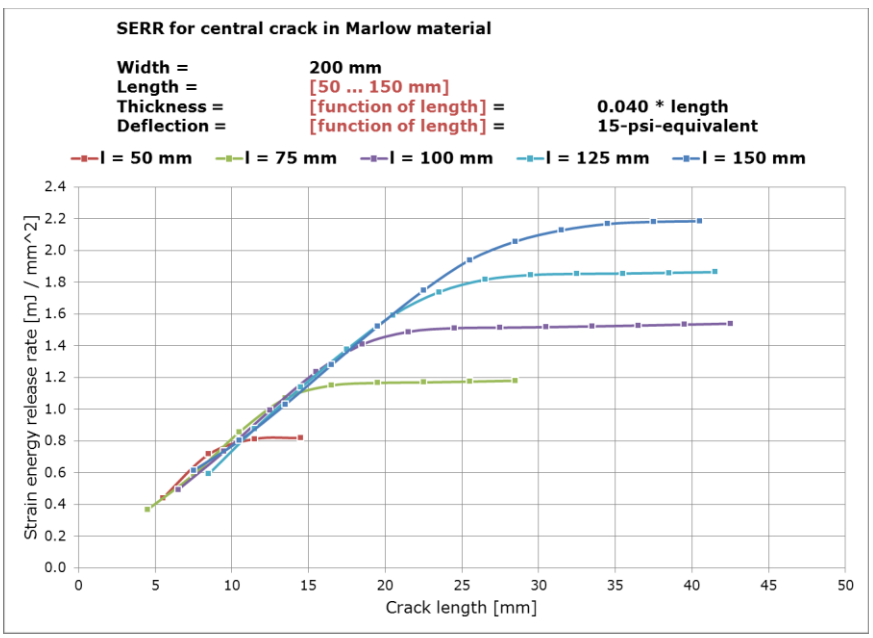

Figure 15. SERR vs. Crack Length, *Variable Length, t = .04*Length.*

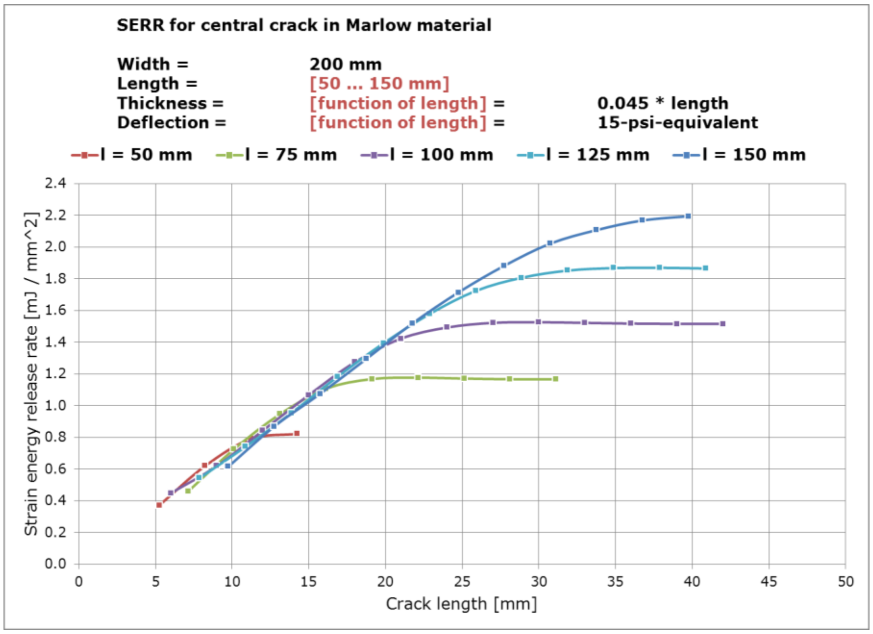

Figure 16. SERR vs. Crack Length, *Variable Length, t = .045*Length.*

4.4 Edge vs. Center Cracks

All of the simulations used to generate the results in Figures 8 through 16 were repeated for the case of two symmetric edge cracks. The edge models were exactly the same as the center crack models except that the symmetry boundary condition was moved from the side of the panel with the crack (as shown in Figure 6) to the opposite side of the panel.

One could argue that a more realistic condition would be to have only one crack present on only one side of the panel. This configuration was checked and the results found to be very close to the symmetric edge crack results.

All in all, the behavior of edge cracks is very similar to central cracks and therefore not shown in detail here. It should be pointed out that, in general, edge cracks cause a slightly higher SERR and that their SERR functions show a less linear shape during phase I where the SERR is dependent on the crack length.

A comparison of the edge vs center crack for the nominal panel under nominal deflection is shown in Figure 17. Note that in the case of the edge crack model, the crack length is the length of one of the two edge cracks. Whereas, in the case of the center crack model, the crack length is the total length of a single center crack.

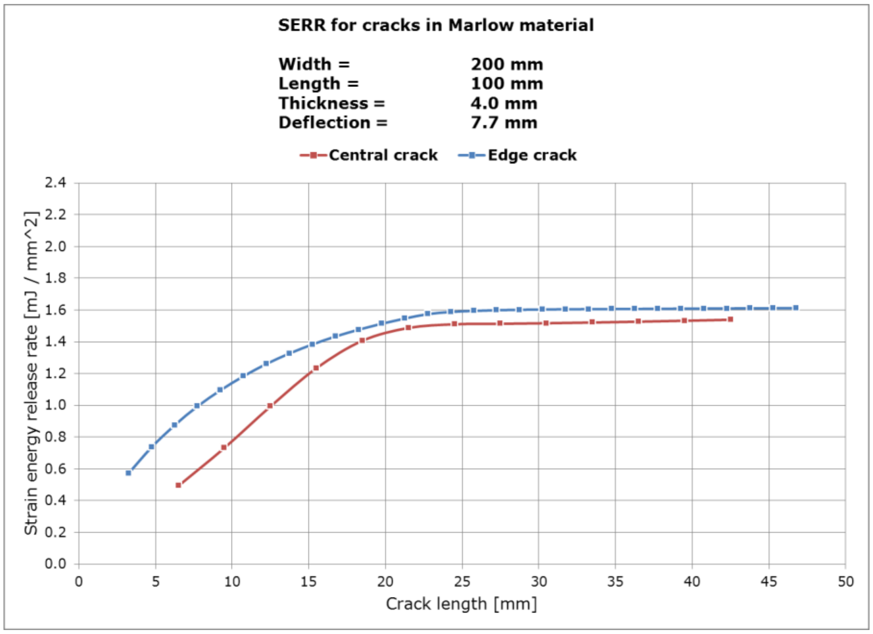

Figure 17. SERR vs. Crack Length, *Center vs. Edge Crack.*

5. Conclusions

This study has shown that crack propagation in compressively flexed elastomeric panels is essentially a two phase phenomenon. During phase I, when the cracks are smaller, the strain energy release rate (SERR) increases with crack length. This increase is nearly linear for central cracks and the slope of this function is controlled mainly by the peak deformation seen by the panel.

By contrast, during phase II, when the cracks are longer, the SERR is no longer strongly dependent on crack length. Rather, the SERR level is controlled mainly by peak strain energy density and panel length. This becomes an especially interesting result when considering the design of very wide compressively flexed panels since it indicates that longer panels are not necessarily the best choice for long life.

6. References

1. R. S. Rivlin, A. G. Thomas, "Rupture of Rubber. I. Characteristic Energy for Tearing", Journal of Polymer Science, Vol. 10, 1953.
2. Abaqus Users Manual, Version 6.11-1, Dassault Systèmes Simulia Corp., Providence, RI., 2011.